Luminescence properties of chalcopyrite $AgInS_2$ nanocrystals: their origin and related electronic states

Yasushi Hamanaka[a)], Tetsuya Ogawa[a)], Masakazu Tsuzuki[a)], Kohei Ozawa[a)], and Toshihiro Kuzuya[b)]

a) *Department of Materials Science and Engineering, Nagoya Institute of Technology, Gokiso-cho, Showa-ku, Nagoya 466-8555, Japan*

b) *College of Design and Manufacturing Technology, Muroran Institute of Technology, 27-1 Mizumoto-cho, Muroran 050-8585, Japan*

E-mail address of each author: hamanaka@nitech.ac.jp (Y. Hamanaka)
t_ogawa@yahoo.co.jp (T. Ogawa)
ciq15057@stn.nitech.ac.jp (M. Tsuzuki)
23415020@stn.nitech.ac.jp (K. Ozawa)
kuzuya@mmm.muroran-it.ac.jp (T. Kuzuya)

Corresponding author: Yasushi Hamanaka
Address: Department of Materials Science and Engineering, Nagoya Institute of Technology, Gokiso-cho, Showa-ku, Nagoya 466-8555, Japan
Tel. +81-52-735-7197
Fax. +81-52-735-7680
E-mail: hamanaka@nitech.ac.jp

Abstract

We report on the photoluminescence (PL) mechanisms of the chalcopyrite $AgInS_2$ nanocrystals with dodecanethiol surfactants. The nanocrystals present broad PL spectra (full width at half maximum of 0.4 eV) with large Stokes-shifts (0.8 – 1.0 eV). Time-resolved PL measurements revealed that the PL decay time depends strongly on the emission energies corresponding to the temporal red-shift of the PL bands. The PL bands also exhibit the blue-shift with increasing excitation intensity. These characteristic behaviors observed in the PL spectra indicate that the luminescence of the $AgInS_2$ nanocrystals originates from the electron-hole pair emission via donor-acceptor pair-like recombination mechanisms. The quantum yield (QY) of PL is up to > 40 % which is at least 4-fold larger compared with QYs reported for other chalcopyrite nanocrystals without ZnS shell (< 10 %), indicating that surface passivation of $AgInS_2$ nanocrystals by dodecanethiol molecules efficiently eliminates surface defects act as non-radiative recombination centers. We conclude that the donor and acceptor states associated with the PL of $AgInS_2$ nanocrystals originate from the lattice defects formed in the interior of nanocrystals, not on surfaces.

Keywords: semiconductor nanocrystal, quantum dot, chalcopyrite, I-III-VI_2, luminescent quantum yield, DA pair recombination

1. Introduction

In recent decades, semiconductor nanocrystals have attracted tremendous attention because of their unique electronic and optical properties and potential utility in applications for future photonic and electronic devices. Most researches have been done in binary semiconductor nanocrystals such as II-VI, I-III, IV-VI, and I-VII types [1,2]. Especially, development of chemical synthesis method of II-VI type nanocrystals such as CdSe and CdS open the way to mass production of size-controlled nanocrystals with highly luminescent properties which have been already used for fluorescent biological labeling [3,4]. However, most of the conventional binary semiconductors contain toxic heavy metals such as Cd, Pb, Hg, As, and Se. Thus, alternative nanocrystals with non-toxic constituents are required from the viewpoint of restriction of hazardous substances.

Recently, to comply with environmental regulations, ternary I-III-VI_2 type (chalcopyrite) nanocrystals such as $CuInS_2$ and $AgInS_2$ have been intensively studied as substitutes for many binary nanocrystals with toxic elements [5-9]. A high photoluminescence quantum yield (PL-QY) of >80 % has been achieved by rapid progresses in fabrication technique of high quality I-III-VI_2 nanocrystals and overcoating them by ZnS layers [10]. Most of the recent research on PL properties of I-III-VI_2 nanocrystals have pointed out that intragap trapping sites due to defects are involved in radiative recombination routes of carriers [7,10-15]. However, detailed PL mechanisms have not been thoroughly elucidated. In this paper, we report on the results of a systematic investigation of the PL properties of chalcopyrite-type $AgInS_2$ nanocrystals by the steady-state and time-resolved PL spectroscopy.

2. Experimental

$AgInS_2$ nanocrystals passivated by dodecanethiol molecules were synthesized via metathesis reaction between metal thiolate and sulfur-dodecanethiol complexes. The details of nanocrystal synthesis are described in Ref.[16]. Nanocrystal diameters (D_{avr}) were controlled by the reaction temperature and changed between 2.5 and 4.3 nm. The chalcopyrite structures and nanocrystal sizes were characterized by x-ray diffraction (XRD) and transmission electron microscope (TEM). The stoichiometry of the nanocrystals was determined by energy dispersive x-ray spectroscopy (EDX). The $AgInS_2$ nanocrystals are slightly S rich with an Ag:In:S ratio of 1:0.91-0.96:2.3-2.7. The excess S content is probably due to the surfactant dodecanethiol molecules on the surface of the nanocrystals.

For steady-state PL measurements, a 532 nm (2.33 eV) line of a continuous wave (CW) Nd:YVO_4 laser was used as an excitation source, and PL spectra were recorded by a 0.45 m monochromator and a cooled CCD detector. In PL decay measurements, a pulsed dye laser pumped by a XeCl excimer laser with a pulse duration of 10 ns operating at 10 Hz was used for excitation. PL was dispersed by a monochromator and decay curves were recorded using a photomultiplier tube and a digital oscilloscope. The QY of PL was determined by comparing the integrated PL intensity of nanocrystals dispersed in hexane to that of the standard dye, rhodamine 101 in ethanol (QY = 96 %), with identical absorbance at the excitation wavelength [17]. The QY was estimated for three different concentrations where the absorbance at the excitation energy is not exceeding 0.1.

3. Results and Discussion

Absorption and PL spectra of $AgInS_2$ nanocrystals with D_{avr} = 2.5, 2.6, 3.4, and 4.3 nm dispersed in hexane are shown in Fig. 1, respectively. A shoulder absorption peak is observed around 2.3 – 2.6 eV in each sample, which is larger than the bandgap energy of bulk $AgInS_2$ with chalcopyrite structure, 1.87 eV [18]. The peak energies of these absorption bands were estimated from the extrema of the second derivative spectra and peak positions are marked by the arrows in Fig. 1. The absorption bands exhibit a blue-shift with decreasing nanocrystal diameter. Such a size-dependent blue-shift of the absorption peak is attributed to a quantum confinement effect of carriers in nanocrystals, and thus, we conclude that the origin of the absorption bands is the transition between the lowest quantized levels of the valence and conduction bands.

The PL spectra show broad emission bands with large Stokes-shifts from the absorption peaks. Such spectral features are typical of type I-III-VI_2 nanocrystals [10-14,16]. Large Stokes-shifts of 0.8 – 1.0 eV and full width at half maximum (FWHM) of about 0.4 eV suggest that the PL is derived from the recombination of electrons and holes where either or both kinds of carriers trapped in intragap levels, not from the transition between the quantized energy levels in conduction and valence bands. A size-dependent blue-shift similar to the absorption bands is also observed in the PL spectra, but the dependence is weak compared with the absorption band because the trapped carriers suffer relatively weak confinement due to their localized nature compared with carriers in the conduction and valence bands.

To understand the detailed PL mechanisms of $AgInS_2$ nanocrystals, we measured the excitation intensity dependence of the PL spectra and the PL decay profiles. PL spectra of $AgInS_2$ nanocrystals were measured with changing excitation intensity by a

factor of $\times 1$ to $\times 10^3$ (0.0027 mW – 2.7 mW). Some of the spectra for nanocrystals with D_{avr} = 2.5, 3.4, and 4.3 nm are picked up and shown in Figs. 2(a), (b) and (c), respectively. As the excitation intensity is increased, the peak of the PL band is shifted to higher energy in any-sized nanocrystals. Figures. 2(d) – (f) show PL decay curves for corresponding nanocrystals in Figs 2(a) – (c) measured at various detection energies in PL bands following pulsed-laser excitation at 2.58 eV. Obviously, the decay times are strongly dependent on the emission energy where the decay is faster for higher emission energies. These characteristics observed in both the excitation-intensity dependence of the PL band and PL decay behaviors are well-known features of a donor-acceptor (DA) pair recombination [19].

In a DA pair recombination, the coulomb interaction between donor and acceptor modifies their binding energies compared to their isolated states. Hence, the photon energy emitted from a DA pair with a separation r is given by the following formula.

$$h\nu = E_g - (E_a + E_d) + e^2/\varepsilon r \qquad (1)$$

Here, E_g is the band-gap energy, and E_a and E_d are the binding energies of the acceptor and donor, respectively, and ε is a dielectric constant. Thus, the emission energy from the nearer pairs is higher than that from the distant pairs, because the coulomb interaction term is larger for nearer pairs. A recombination between nearer pairs is more probable than a recombination between distant pairs due to greater wave function overlap, which results in faster decay for higher emission energies in the PL band. Such decay behavior leads to the temporal red-shift of the PL spectrum. In addition, the contribution of nearer pairs with large recombination probability becomes dominant in a DA pair emission process under high intensity excitation, while the contribution of distant pairs is relatively larger under low intensity excitation. This is because only a fraction of the donors and acceptors are excited under low excitation condition and hence only distant pairs recombine while at high excitation intensity most of the donors and acceptors are excited and nearer pairs also recombine. Therefore, the PL spectrum exhibits blue-shift with increasing excitation intensity. Both of them coincide well with PL characteristics shown in Fig. 2.

Temporal behaviors characteristic of the DA pair emission are obviously represented in time-resolved PL spectra. Time-resolved PL spectra can be constructed from the PL decay curves measured at various detection energies. Those of $AgInS_2$ nanocrystals with D_{avr} = 2.6 nm are shown in the inset of Fig. 3 for delay times of 0 and 1 μs. The peak of the PL spectrum is found to be shifted to lower energy and the

high-energy component of the PL spectrum is reduced at 1 μs after the excitation. The peak energies and FWHMs of the time-resolved PL spectra were estimated by spectral fitting analysis assuming a Gaussian profile of PL bands, and their time-evolutions are shown in Fig. 3. Peak energy decreases down about 0.09 eV in the first 1 μs time delay, and the FWHM simultaneously decreases from 0.46 to 0.31 eV. Such a temporal behavior of the PL spectrum is interpreted in terms of higher recombination rate of the nearer DA pairs and strong evidence of the DA pair emission. Therefore, we conclude that the PL mechanisms of $AgInS_2$ nanocrystals is ascribed to the pair recombination of electrons and holes trapped at defect sites with donor and acceptor characters.

Although the contribution of the distant pairs in the nanocrystals is dominant in the PL spectrum at the long delay time in DA pair emission, the PL spectra of $AgInS_2$ nanocrystals are still broad for the long delay time as shown in Fig. 3. Similar broad PL spectra with large Stokes-shift assigned to the DA pair recombination were also observed in CdS and CdSe nanocrystals and [20,21]. Such spectral profiles were ascribed to the strong carrier-phonon interaction due to deeply trapped carriers at defect sites located on the surface. Large Huang-Rhys factors (110 for CdS and 18 for CdSe) were deduced from spectral shapes, indicating that the phonon sidebands constitute the dominant contribution to the entire PL spectra. Both the large spectral width and large Stokes-shift observed in the PL spectra of $AgInS_2$ nanocrystals may be also attributed to the strong carrier-phonon interaction.

Figures. 2(d) – (f) show that an additional decay component with shorter decay times of < 200 ns appears at emission energies corresponding to the high energy tail of the steady state PL spectra, while the decay curves for relatively low emission energies exhibit nearly single-exponential profile with decay times of microsecond to sub-microsecond scale. This short-lived component may not originate from the pair recombination process but from the other recombination processes such as a near-band-edge emission. Further experiments on the PL dynamics are required to determine the origin of the entire PL spectrum of $AgInS_2$ nanocrystals.

The donor and acceptor states concerning to the electron-hole pair emission of $AgInS_2$ nanocrystals may have their origin in surface defects that act as trap sites for carriers similar to CdS and CdSe nanocrystals mentioned above and/or in intrinsic lattice defects such as vacancies, interstitial atoms, and antisite defects formed in the interior of nanocrystals. The PL-QYs of the as-synthesized chalcopyrite nanocrystals are usually below 10 % [10,11,13-15]. The QYs increase and exceed 60 % by capping the nanocrystals with ZnS layers [10,13,15]. The remarkable enhancement of the QYs is interpreted as elimination of the surface defects which mainly act as the non-radiative

recombination centers. In the present study, the PL-QY of $AgInS_2$ nanocrystals with D_{avr} = 2.6 nm was estimated to be 46 %, which is exceptionally high among as-synthesized chalcopyrite nanocrystals without ZnS capping. The high QY represents that less amount of the surface defects remains in these nanocrystals due to the surface passivation by dodecanethiol molecules, and thus, implies that the PL does not originate from the surface defects but from the intrinsic defects inside of nanocrystals. In bulk chalcopyrite $AgInS_2$, vacancies and interstitial atoms of sulfur and silver are formed as native defects. These defects have donor- and acceptor-characters and act as trapping centers in DA pair emission [22]. It is probable that similar defects are formed in the interior of $AgInS_2$ nanocrystals and provide the electron-hole pair emission.

We have also estimated the PL-QY of CdSe/ZnS core/shell-type nanocrystals commercially provided by Aldrich (Lumidot 610) by the same method. The QY is determined to be 36 %, which is coincident with the QY of 30 – 50 % ensured from the supplier. In Fig. 4, PL spectra of the CdSe/ZnS nanocrystals and $AgInS_2$ nanocrystals with almost the same concentrations are shown together with the absorption spectra. The PL of the CdSe/ZnS nanocrystals is due to the exciton recombination, therefore the spectrum is relatively sharp compared with the $AgInS_2$ nanocrystals. But the $AgInS_2$ nanocrystals without ZnS shell investigated in this study exhibit high PL-QY comparable to CdSe/ZnS nanocrystals. Therefore, chalcopyrite $AgInS_2$ nanocrystals represent potential for alternative materials to cadmium-based nanocrystals in applications such as light-emitting devices and fluorescent biological tags used in vivo.

4. Conclusion

Chalcopyrite $AgInS_2$ nanocrystals passivated by dodecanethiol molecules with average diameters of 2.5 – 4.3 nm were synthesized and their PL properties were investigated. The absorption and PL peak energies shift to higher energy as the nanocrystal size decreases due to a quantum confinement effect of carriers in nanocrystals. The PL bands are broad and exhibit large Stokes-shifts, and ascribed to the DA pair-like recombination of carriers because of the excitation intensity dependence of the PL peak energy and the wide variation in the PL decay times depending on the emission energy. The PL-QY is estimated to be 46 %, to our best knowledge, which is the highest value among as-synthesized I-III-VI_2 type nanocrystals without ZnS capping layers. Such a high PL-QY implies that creation of the surface defects act as nonradiative recombination centers is sufficiently suppressed by surface passivation. Consequently, lattice defects with donor- and acceptor-characters are formed in the interior of $AgInS_2$ nanocrystals and provide major contributions in the electron-hole pair

emission.

Acknowledgements

The authors are grateful to Professor K. Sumiyama for technical supports and discussions at the beginning of this study. This work was partly performed in Nanotechnology Support Project in Central Japan financially supported by Nanotechnology Network of the Ministry of Education, Culture, Sports, Science and Technology (MEXT), Japan.

References

[1] Y. Masumoto, T. Takagahara, Semiconductor Quantum Dots: Physics, Spectroscopy, and Applications, Speringer, Berlin, 2002.

[2] H. S. Nalwa, Nanostructured Materials and Nanotechnology, Academic Press, San Diego, 2002.

[3] B. H. Weller, Angew. Chem. Int. Ed. Engl. 32 (1993) 41.

[4] M. Bruchez Jr., M. Moronne, P. Gin, S. Weiss, A. P. Alivisatos, Science 281 (1998) 2013.

[5] S. L. Castro, S. G. Bailey, R. P. Raffaelle, K. K. Banger, A. F. Hepp, Chem. Mater. 15 (2003) 3142.

[6] L. Tian, H. I. Elim, W. Ji, J. J. Vittal, Chem. Commun. 41 (2006) 4276.

[7] T. Kino, T. Kuzuya, K. Itoh, K. Sumiyama, T. Wakamatsu, M. Ichidate, Mater. Trans. 49 (2008) 435.

[8] F. M. Courtel, R. W. Paynter, B. Marson, M. Morin, Chem. Mater. 21 (2009) 3752.

[9] R. Xie, M. Rutherford, X. Peng, J. Am. Chem. Soc. 131 (2009) 5691.

[10] J. Li, A. Pandey, D. J. Werder, B. P. Khanal, J. M. Pietryga, V. I. Klimov, J. Am. Chem. Soc. 133 (2011) 1176.

[11] S. L. Castro, S. G. Bailey, R. P. Raffaelle, K. K. Banger, A. F. Hepp, J. Phys. Chem. B108 (2004) 12429.

[12] Y. Hamanaka, T. Kuzuya, T. Sofue, T. Kino, K. Ito, K. Sumiyama, Chem. Phys. Lett. 466 (2008) 176.

[13] M. Uehara, K. Watanabe, Y. Tajiri, H. Nakamura, H. Maeda, J. Chem. Phys. 129 (2008) 134709.

[14] H. Zhong, Y. Zhou, M. Ye, Y. He, J. Ye, C. He, C. Yang, Y. Li, Chem. Mater. 20 (2008) 6434.

[15] B. Mao, C-H. Chuang, J. Wang, C. Burda, J. Phys. Chem. C115 (2011) 8945.

[16] T. Ogawa, T. Kuzuya, Y. Hamanaka, K. Sumiyama, J. Mater. Chem. 20 (2010) 68.

[17] R. F. Kubin, A. N. Fletcher, J. Lumin. 27 (1982) 455.

[18] J. L. Shay, J. H. Wernick, Ternary Chalcopyrite Semiconductors: Growth, Electronic Properties, and Applications, Pergamon Press, Oxford, 1975.

[19] P. Y. Yu, M. Cardona, Fundamentals of Semiconductors: physics and materials properties, Springer, Berlin, 1999.

[20] N. Chestnoy, T. D. Harris, R. Hull, L. E. Brus, J. Phys. Chem. 90 (1986) 3393.

[21] E. Lifshitz, I. Dag, I. Litvin, G. Hodes, S. Gorer, R. Reisfeld, M. Zelner, H. Minti, Chem. Phys. Lett. 288 (1998) 188.

[22] S. H. You, K. J. Hong, C. J. Youn, T. S. Jeong, J. D. Moon, H. S. Kim, J. S. Park, J.

Appl. Phys. 90 (2001) 3894.

Figure Captions

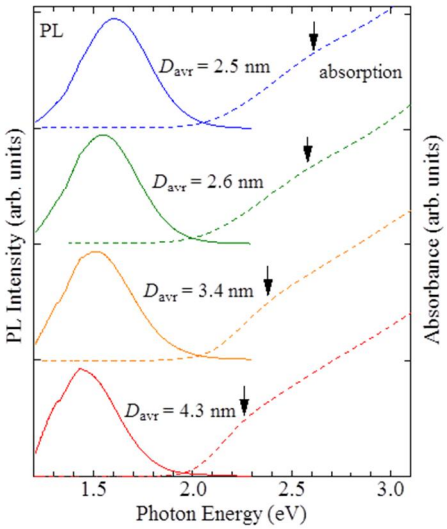

Figure 1. Y.Hamanaka et al.

Fig. 1 Absorption spectra (dashed curve) and PL spectra (solid curve) of $AgInS_2$ nanocrystals dispersed in hexane.

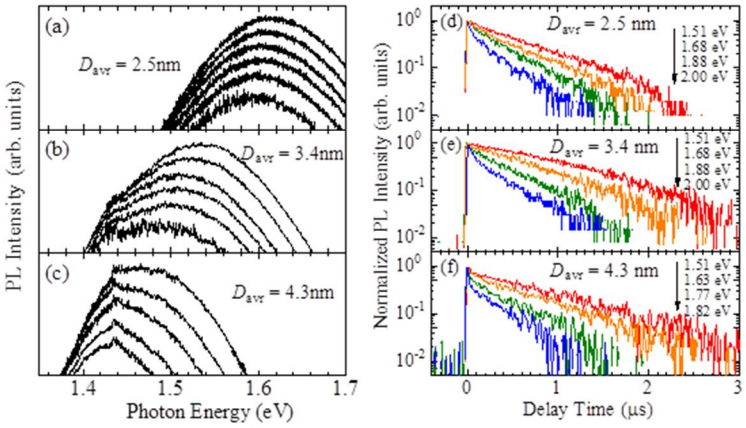

Figure 2. Y.Hamanaka et al.

Fig. 2 (a) – (c) PL spectra of $AgInS_2$ nanocrystals measured with different excitation laser intensities between 2.7 mW and 0.0027 mW (from top to bottom). (d) – (f) PL decay curves of $AgInS_2$ nanocrystals detected at different emission energies. Average diameters of $AgInS_2$ nanocrystals are 2.5 nm ((a) and (d)), 3.4 nm ((b), (e)), and 4.3 nm ((c), (f)), respectively.

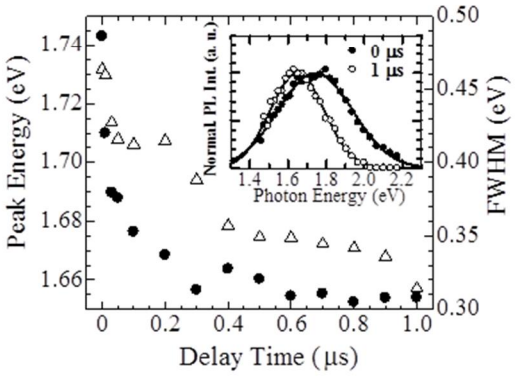

Figure 3. Y.Hamanaka et al.

Fig. 3 Time evolution of the peak energies (circles) and FWHMs (triangles) of the PL bands of $AgInS_2$ nanocrystals with D_{avr} = 2.6 nm. The inset shows the time-resolved PL spectra measured at 0 μs and 1 μs after the excitation. The solid lines in the inset represent the results of the spectral fitting analysis.

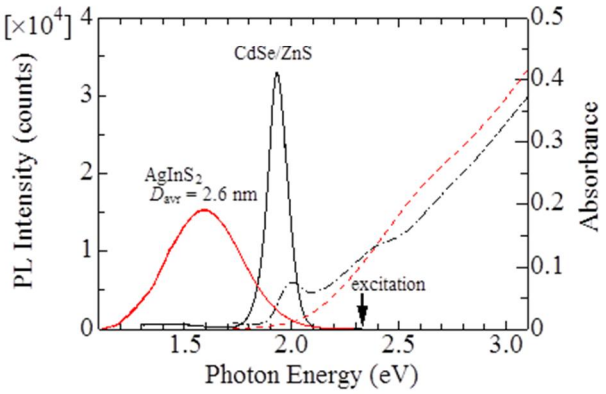

Figure 4. Y.Hamanaka et al.

Fig. 4 Absorption spectra of $AgInS_2$ nanocrystals with D_{avr} = 2.6 nm (dashed curve) and CdSe/ZnS core/shell nanocrystals (Aldrich Lumidot 610, dot-dashed curve), and their PL spectra (solid curves) with the same absorbance at the excitation energy, 2.33 eV.